



## Polyhydroxybutyrate/hemp biocomposite: tuning performances by process and compatibilisation

François Touchaleaume, Romain Tessier, Rémi Auvergne, Sylvain Caillol,  
Sandrine Hoppe, Helene Angellier-Coussy

### ► To cite this version:

François Touchaleaume, Romain Tessier, Rémi Auvergne, Sylvain Caillol, Sandrine Hoppe, et al.. Polyhydroxybutyrate/hemp biocomposite: tuning performances by process and compatibilisation. Green materials, 2019, 7 (4), pp.194-204. 10.1680/jgrma.19.00005 . hal-02196923

**HAL Id: hal-02196923**

**<https://hal.science/hal-02196923>**

Submitted on 7 May 2020

**HAL** is a multi-disciplinary open access archive for the deposit and dissemination of scientific research documents, whether they are published or not. The documents may come from teaching and research institutions in France or abroad, or from public or private research centers.

L'archive ouverte pluridisciplinaire **HAL**, est destinée au dépôt et à la diffusion de documents scientifiques de niveau recherche, publiés ou non, émanant des établissements d'enseignement et de recherche français ou étrangers, des laboratoires publics ou privés.

**Biocomposites from polyhydroxybutyrate and hemp fibres: Effects of processing and compatibilizer on structure/performance relationships**

François Touchaleaume<sup>1,2,\*</sup>, Romain Tessier<sup>3</sup>, Rémi Auvergne<sup>2</sup>, Sylvain Caillol<sup>2</sup>, Sandrine Hoppé<sup>3</sup>, Hélène Angellier-Coussy<sup>1</sup>

<sup>1</sup> JRU IATE 1208 – CIRAD/INRA/Montpellier SupAgro/University of Montpellier, 2 place Pierre Viala, F-34060 Montpellier, France

<sup>2</sup> Institut Charles Gerhardt, CNRS, ENSCM, Université de Montpellier - Montpellier - France

<sup>3</sup> University of Lorraine - CNRS, Reaction and Process Engineering Laboratory - Nancy - France,

\*corresponding author: [francoistouchaleaume@gmail.com](mailto:francoistouchaleaume@gmail.com)

Code de champ modifié

## Abstract

A fully bio-sourced and biodegradable composite materials has been developed, based on polyhydroxybutyrate and hemp fibres (20wt% content). Improvements of the final performances of composite materials are not only related to the filler content and intrinsic properties of constituents, but also to the filler dispersion state and to the filler/matrix interface. Hence, the weak interactions between the apolar matrix and the polar fibres have been counterbalanced by adding a green compatibilizer. The impact of processing (screw profile and speed) and formulation (compatibilizing route) on the structure and thermal properties of biocomposites has been discussed in relation to their mechanical properties and water vapour sensitivity. A strong nucleating effect provided by the fibres has been highlighted and a clear fibre-matrix load transfer confirmed the effectiveness of the prepared compatibilizer. Biodegradability of those fully biobased composites was also evaluated in compost.

**Keywords:** A-Polymer-matrix composites, A-Natural fibres, B-Mechanical properties, E-Extrusion

## 1. Introduction

Biocomposites based on the combination of both bio-sourced and biodegradable polymer matrices and vegetal fillers have been extensively developed during the last decade in response to environmental concerns and/or to develop specific new functionalities. Among promising bioplastics, polyhydroxyalkanoates (PHAs), such as polyhydroxybutyrate (PHB), bacterial aliphatic copolyesters fully biodegradable materials [1, 2] that can be produced from food industry by-products [3], agricultural or urban waste [4, 5]. Short lignocellulosic fibres stemming from jute [6], hemp [6, 7], wheat straw fibres [8, 9], olive pomace [8], coffee waste [10] or potato peel waste fermentation residues [11] can be incorporated in such way as to

decrease the overall cost of PHA-based materials and open their window of applications by modulating their functional properties.

One of the main bottlenecks of PHB/lignocellulosic fibres biocomposites is the poor affinity between lignocellulosic fibres and PHB resulting in limited tensile properties. To overcome this problem, different strategies can be applied to improve wettability and intimate contact between lignocellulosic fibres and polymer matrices, *i.e.* the fibre surface modification to increase their surface free energy and particularly their hydrophobicity, the polymer matrix modification to increase its hydrophilicity, or the introduction of amphiphilic compatibilizers [12-15]. If the incorporation of compatibilizers is widely reported in literature, particularly using melt extrusion [16], only a handful of papers depict the use of bio-based compatibilizers [17], while biosourcing plasticizers has become a common practice [18]. A combination of biobased polyethylene-graft- maleic anhydride (PE-g-MA) with sepiolite was proposed by Samper-Madrigal et al. to manufacture films made of polyethylene and 30 wt% of thermoplastic starch (TPS) [19]. Some authors proposed glycolysis of polylactide (PLA) with biobased polyols such as glycerol or sorbitol to yield compatibilizer oligomers to enhance compatibilization in PLA/starch composites [20]. Recently, Xiong et al. [21] proposed the epoxidization of bio-based cardanol with epichlorohydrin to yield an effective bio-based compatibilizer for PLA/starch composites.

Our team proposes a new strategy to synthesize bio-based compatibilizers for PHB/hemp fibre composites. We intend to design oligo-PHB with aromatic groups, which could develop interactions with hemp fibres, by depolymerizing PHB with alcohol functions of biobased aromatic groups. Our team deeply studied cardanol [22] or tannins [23], which only bear phenol groups, and also lignin derivatives including vanillin and vanillin alcohol, which have a primary alcohol that could be a good candidate to depolymerize PHB. Indeed, vanillin and derivatives are especially interesting as vanillin is the only mono-aromatic compound currently industrially

produced from lignin [23, 24]. In a previous paper [25], our team investigated the functionalization of vanillin and its derivatives at different oxidation states.

In addition to this chemical strategy that reduces the lack of affinity between the components, it is necessary to homogeneously disperse the fibres within the polymer the matrix to fully benefit from the introduction of fibres. For that purpose, processing conditions need to be optimized as largely reported in the literature, whatever the fibre type [26-28]. Ranganathan et al. recently reported that when manufacturing viscose fibre/PP composites at low shear, the fibre bundles retained in clusters, whereas higher shear conditions drove to homogenized fibre dispersion and higher mechanical performances. Further addition of dispersing agent improved the fibre dispersion along with the mechanical performance of the composites [29]. Similarly, Kuroda and Scott performed basic experiments concerning the dispersion mechanism of glass fibre bundles and found that complete dispersion occurs above a critical shear stress [30].

The objective of the present work is to optimize the mechanical performance of PHB/hemp fibres biocomposites by investigating and combining two routes: 1/ extrusion processing conditions (screw profile and speed) and 2/ addition of bio-based compatibilizers produced by reactive melt extrusion from the depolymerization of PHB with vanillin alcohol. The impact of processing and formulation on mechanical properties, water vapour sensitivity and biodegradability has been assessed and discussed in relation to the structure of the materials.

## **2. Materials and methods**

### **2.1. Raw materials**

A commercial polyhydroxybutyrate (PHB) was purchased from Metabolix, Germany (P(3HB-co-4HB) with 5% of 4-hydroxybutyrate, M2100 grade). Pellets were vacuum dried overnight at 60 °C before processing. Hemp fibres (retted, carded, 4mm long) were provided by

Chanvriers de l'Est (France). Zinc acetate dihydrate (ZnAc2, 99% of purity) and vanillic alcohol (VA, 98% of purity) were purchased from Sigma-Aldrich.

## 2.2. Synthesis of the compatibilizer

The compatibilizer was obtained by trans-esterification of PHB by VA in a batch-way. In a two-neck flask, PHB and VA were mechanically stirred and heated at 180°C with ZnAc2 as a trans-esterification catalyst (1w% relative to polymer) in order to obtain oligo-esters exhibiting a phenol end (Figure 1). Reagents were previously dried for one night at 45°C in a vacuum oven and three argon/vacuum cycles were applied to the flask prior to heating so as to remove residual oxygen. Reaction was maintained during 1.5 hour and the material was then put in a vacuum container during cooling and further hand-crushed in a mortar.

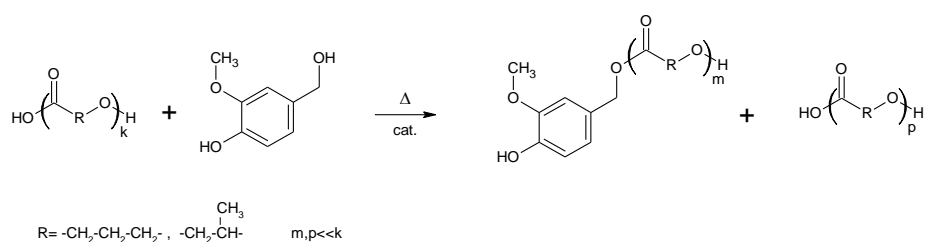


Fig. 1 Trans-esterification of PHB by vanillic alcohol

A masterbatch of the compatibilizer previously prepared was compounded in a Eurolab 16XL twin screw extruder (ThermoScientific). Pellets of compatibilizer and P(3HB-co-4HB) were previously dry mixed, the coupling agent standing for 30w% of the total throughput (2.86 kg.h<sup>-1</sup>). Both components were dried before extrusion and screw speed was set at 500 rpm, leading to a residence time of 70-75 s. The temperature profile was a downstream gradient from 180°C at the feeder to 150°C at the die. The so prepared masterbatch was air dried and further pelletized.

## 2.3. Preparation of PHB/hemp fibres biocomposites

Pellets of virgin PHB and compatibilizer masterbatch were dried for one night in a vacuum oven at 45°C and mixed in a plastic can before processing. Biocomposites were prepared in a twin-screw extruder with a L/D ratio of 28 and a screw diameter of 24 mm (Haake PolyLab, Thermo Scientific). Hemp fibres were dried at 80°C for 1 hour and added to the extruder by a lateral feeder directly into the polymer/masterbatch melt. The fibre content was set at 20%, the temperature was set at 180°C all along the screw and the total throughput was 4.5 kg.h<sup>-1</sup>.

Three screw speeds were chosen (250, 500 and 750 rpm) and two screw profiles have been tested providing two different shear levels to the extruded material. The first screw profile was constituted by five distributions zones (made of mixing elements) and one single dispersion zone (made of mixing elements directly followed by an inverse screw thread) and was called “Low Shear profile”. The second screw profile was constituted by five dispersion zones and one distribution zone and called “High Shear profile”. Residence times for the Low Shear profile were 80 s, 50 s and 40 s at 250 rpm, 500 rpm and 750 rpm, respectively. When using the High Shear profile, the residence times were 115 s, 90 s and 80s when processing at 250 rpm, 500 rpm and 750 rpm, respectively.

Extruded composites were granulated, dried for one night in a vacuum oven at 45°C and further injected as dog-bone samples with the aid of a DSM MC15 microcompounder and a DSM IM12 injection moulding machine. Mould geometries were chosen according to ISO 572-2 standard specifications and injected samples were of 1B type. It is worth noting that unfilled materials could not be processed along with this last step as injection molding requires crystallizing kinetics that those compositions did not show since no crystallization agent was employed. Samples were codified as follows: with compatibilizer: PHB-C-H; without: PHB-H. Processing conditions are ~~precised-detailed~~ as follow: “LS” and “HS” referring to the materials elaborated with the low shear and the high shear profiles, respectively. The three digits’ figure of the sample codification refer to the screw speed chosen during processing, in rpm.

## **2.4. Characterization of PHB/hem fibres biocomposites**

### **Scanning Electron Microscopy.**

Scanning electron microscopy (SEM) observations were performed using a scanning electron microscope (SEM S-4500, Hitachi, Japan) with an acceleration voltage of 2 kV and a detector for secondary electrons. Prior to observation, the injection molded samples were frozen under liquid nitrogen, then fractured, mounted and coated with gold on an ion sputter coater.

### **Molecular weight analysis.**

The weight-average molecular weights ( $M_w$ ) were determined by gel permeation chromatography (GPC) on a Waters HPLC system equipped with a Waters 410 differential refractive-index detector, a 600 mm column PL gel MixC 5 $\mu$ m. The mobile phase was  $\text{CHCl}_3$ , its flow rate set at 0.8ml/min at 30°C and toluene used as flowmarker. The samples were prepared as 10mg/ml solutions and when containing fibres, were filtered on a 45  $\mu$ m-pores filter (VWR, filter paper, qualitative 413). Then, all samples were filtered using 0.2 $\mu$ m PTFE filters. A sample injection volume of 200  $\mu$ L was used in the GPC analysis and the calibration was performed with PS standards.

### **Differential Scanning Calorimetry.**

Differential Scanning Calorimetry (DSC) measurements were performed with a calorimetric NETZSCH DSC 200 F3 calibrated with an indium standard. Samples of  $10 \pm 2$  mg were placed in the measurement heating cell and were heated under inert atmosphere from  $-50$  to  $200$  °C at a heating rate of  $20$  °C/min. Two heating runs and a cooling one were recorded and the glass transition temperature ( $T_g$ ) values were measured during the second run.  $T_g$ s were calculated

at the mild point of the heat capacity jump. The crystallinity degree was obtained from the DSC curve using the following equation:

$$\frac{\Delta H_m - \Delta H_{cc}}{\Delta H_{m100\%} \times (1 - \alpha)}$$

where  $\Delta H_m$  is the measured melting enthalpy for a given sample,  $\Delta H_{cc}$  the cold crystallization enthalpy,  $\Delta H_{m100\%}$  the melting enthalpy of 100% crystallized PHB (144 J/g) [31] and  $(1 - \alpha)$  is the weight fraction of polymer in the material.

#### **Thermal stability. ATG**

Thermogravimetric analyses (TGA) were performed on a Q50 from TA Instrument. 10 mg of sample were displayed in an aluminum pan and heated from RT to 550°C under a nitrogen flow (60 mL/min). The experiments were carried out at a heating rate of 10°C/min.

#### **Tensile tests.**

Mechanical tensile tests were performed on a Zwick metrology Z010 apparatus owing to NF EN ISO 527-1 standard in order to determine mechanical properties of materials. The apparatus is equipped with pneumatic grips, with 100 mm spacing, a sensor of 500 N or 5 kN depending on the tested materials. Traction speed is 10mm/min, controlled by position regulation, with a preload of 2 N before measurement. Results are an average of measurements performed on at least five samples.

#### **Water sorption kinetics.**

Moisture sorption isotherms were determined with the aid of a precision scale. The experiments were carried out on end-parts of dog-bone injection molded samples. The samples were dried at 40 °C in a vacuum oven for 24 hours and then let to equilibrate at 0% relative humidity (RH) for one week before measurement. The sorption curves were conducted at 25°C with 96 RH%. The moisture uptake  $M(t)$  was calculated using the following equation:

$$M(t) = \frac{w_{moist}(t) - w_{dry}}{w_{dry}} \times 100$$

where  $w_{moist}(t)$  is the sample weight exposed to 96 RH% for a time  $t$  and  $w_{dry}$  is the dry weight of the sample at 0 RH%. Numerous models have been developed to properly describe the moisture contamination of composite materials [32, 33]. As indicated in the ASTM standard for water diffusion in thin plates of fibre-reinforced polymers [34], this process can be adequately described by the one dimensional Fick's second law:

$$\frac{\partial c}{\partial t} = D \frac{\partial^2 c}{\partial x^2}$$

where  $c$  is the moisture concentration,  $D$  is the diffusion coefficient,  $t$  is the time and  $x$  is the position through the thickness. A useful closed-form approximate solution is given as [35]:

$$\frac{M(t)}{Ms} \approx 1 - \exp \left[ -7.3 \left( \frac{Dt}{h^2} \right)^{0.75} \right]$$

where  $M(t)$  is the evolution of the water absorbed,  $Ms$  the water content at saturation and  $h$  the thickness of the plate. The curve were fitted thanks to a Levenberg-Marquardt algorithm applied on the asymptotic model performed on OriginPro 2017 software. All the ~~coefficients~~coefficients of determination ( $r^2$ ) were higher than 0.993.

### **Biodegradation.**

Respirometric tests were conducted in compost medium at 58°C to evaluate the biodegradability of the materials. The method was adapted from the US standard ASTM D5988-03 to determine the Aerobic Biodegradation of Plastic Materials After Composting. The released CO<sub>2</sub> being proportional to the percentage of biodegraded substrate, CO<sub>2</sub> evolution quantifies the ultimate degradation step (*i.e.* mineralization) during which a substance is broken down to its final products [36]. Beforehand, materials were cut into 1-2mm bits and carbon contents were measured with an elementary ~~analyser~~analyzer (ThermoQuest NA 2500) in order

to precisely set the material dose to 50 mg of carbon into 3g of compost. Biodegradation tests were carried out in real and mature compost. Distilled water was initially added to the solid media and then regularly added all along the experiment to maintain the moisture content of the medium around 80–100%.

### **3. Results and discussion**

#### **3.1. Multi-scale structure of PHB/hemp fibres biocomposites**

##### ***3.1.1. Morphology of composite samples***

The morphology of PHB-based composites was assessed by SEM observations of cryo-fractured surfaces of injected samples (figure 2). Such observations gave information on two aspects of the impact of the elaboration conditions on the microstructure of the prepared composites. The first one was the dispersion state of the fibres which is mainly influenced by the shear applied to the melt during extrusion and which could be assessed at low magnification (figures 2a and 2b). Dispersion of the hemp fibres within the PHB matrix appeared homogeneous. The absence of fibre cluster was an encouraging indicator for favored interactions between the matrix and the fibres. However, no significant impact of the processing conditions was picked up. Indeed, the composite prepared under the most severe conditions, i.e. using the high-shear profile at 750 rpm (figure 2a) exhibited a fibre dispersion as uniform as the one prepared under the softest conditions, i.e. the low-shear profile at 250 rpm (figure 2b), indicating that the shearing forces induced by all the chosen processing conditions were sufficient enough to homogeneously dispersed hemp fibres within the polymer matrix.

The second investigated characteristic of the microstructure was the level of interfacial adhesion between the matrix and the fibres, usually influenced by the chemistry of the environment. This was qualitatively assessed by high magnification observations of the filler/matrix interface. Figures 2c and 2d exhibit pictures of two composites elaborated with

similar processing conditions (high-shear profile, 250 rpm), leading to the highest residence time of the various processing conditions. The reported pictures revealed dissimilar fibre/matrix adhesion levels whether a compatibilizer had been added or not. The composite prepared with a compatibilizer (figure 2d) exhibited an interphase between the fibre and the polymer, while gaps could be noticed between the hemp fibres and the matrix when no compatibilizer was employed (figure 2c). This improvement of the interface revealed that this residence time (115 s) was long enough to develop an interphase, confirming thus the efficiency of the compatibilizer. However, all the compatibilized materials (PHB-C-H) exhibited quite similar dispersion states and interphases, whatever the residence time, *i.e.* whatever the processing conditions employed. Nevertheless, even if those various materials could not be discriminated by SEM analyses, their performances could also be linked to their macromolecular structure and molar masses.

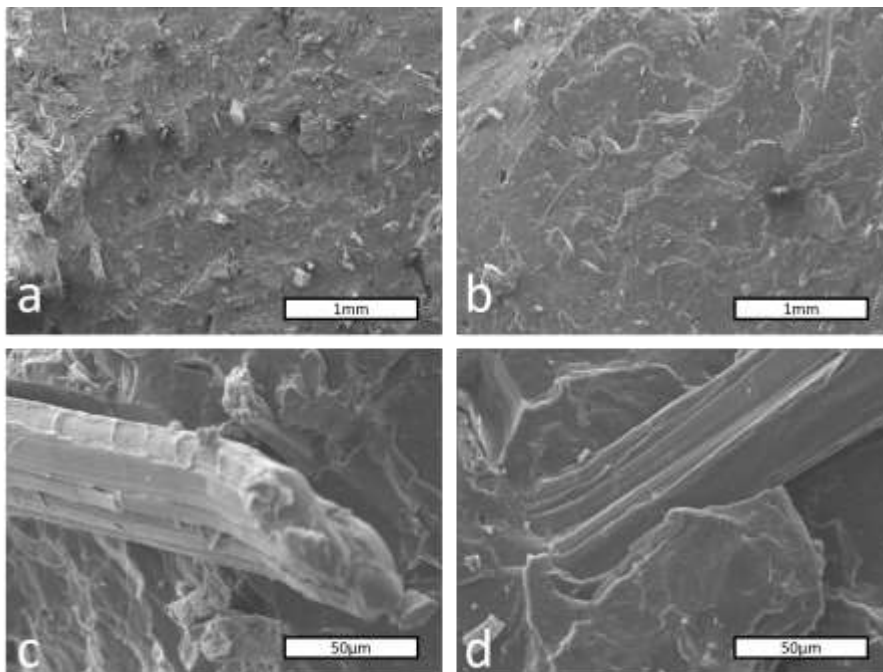


Fig. 2. SEM pictures of PHB-hemp fibres composites elaborated under extreme shears (a: PHB-H HS750; b: PHB-H LS250) and with the highest residence time (c: PHB-H HS250; d: PHB-C-H HS250)

### 3.1.2. Polymer molar mass

Molar mass analyses have been performed on the injection-molded biocomposites prepared under various processing conditions and with various compositions (Table 1). The pristine PHB matrix displayed a molar mass ( $M_w$ ) of  $150,700 \text{ g.mol}^{-1}$ . In comparison with this reference value, all samples underwent a common reduction of the molar mass when the material was submitted to an extra processing step (Table 1). This reduction was comprised between -13% for the virgin PHB extruded under the softest conditions (LS250) down to -71% for the PHB-C-H extruded under the most severe processing conditions (HS750). More precisely, when comparing the two screw profiles at a similar screw speed, the  $M_w$  drop was stronger for the material processed with the high shear profile with the low shear one (table 1). For instance, the two PHB-H materials processed at 250 rpm reveal  $M_w$  equal to  $122,200 \text{ g.mol}^{-1}$  and  $72,200 \text{ g.mol}^{-1}$  with the low-shear and the high-shear profiles respectively, corresponding to a 19% reduction for the low-shear processed material and to a 49% reduction for the high-shear processed one, in comparison with pristine PHB. Those  $M_w$  reductions were even more pronounced when the screw speed increased (in spite of reduced residence times). Indeed, the molar mass decreased from  $122,200 \text{ g.mol}^{-1}$  for the PHB-H processed with the low-shear profile down to  $63,700 \text{ g.mol}^{-1}$  when the screw speed was increased from 250 rpm up to 750 rpm. This sensitivity to mechanical stresses exhibited by polyester-based materials has already been widely studied [37-40]. Literature also reports a decisive role played by moisture during extrusion, inducing hydrolysis reactions [38]. When adding fibres, two phenomena contributed to worsen this  $M_w$  drop: 1/ PHB hydrolysis was favored by the presence of water, alcohols

and/or acids produced during biomass thermal degradation [8, 41], 2/ melt shear viscosity was higher than without fibre, increasing then the internal warming during the process of thermally sensitive PHB. When the compatibilizer was introduced, PHB-C-H exhibited slightly lower Mw than the corresponding PHB-H. For instance, the composites processed at 250 rpm under low-shear exhibit a molar mass of 122,200 g.mol<sup>-1</sup> without compatibilizer and 106,500 g.mol<sup>-1</sup> when 2.4 wt% compatibilizer was added, indicating a 18.9% reduction for PHB-H and 29.3% reduction for PHB-C-H. This increase of degradation level induced by the presence of the compatibilizer was expected as the composite processing conditions were similar to those of the compatibilizer synthesis (transesterification in reactive extrusion with catalyzer still in media). The required experimental conditions being fulfilled, the transesterification reaction occurred during the compounding process, thus favoring an extra reduction of the PHB molar mass.

**Table 1.** Thermal (Tg: glass transition; Tm: melting temperature; Tc: crystallization temperature; T-5%: degradation onset) and molecular (Mw: mass-average molar mass; Xc: crystallinity) properties of PHB-based materials.

Screw profile	Screw speed	Sample	Mw (kg/mol)	Tg (°C)	Tm(°C)	Xc(%)	Tc(°C)	T-5% (°C)
-	-	PHB as received	150.7	4	174	3.6	ind.	280
Low Shear Profile	250 rpm	PHB	130.7	3	171	9.6	0-50°C	265
	250 rpm	PHB-H	122.2	0	171	41.8	78	258
	500 rpm	PHB-H	90.0	1	170	37.2	76	258
	750 rpm	PHB-H	63.7	-1	167	37.8	76	254
	250 rpm	PHB-C-H	106.5	1	171	40.7	76	258
	500 rpm	PHB-C-H	80.6	3	170	40.0	74	259
	750 rpm	PHB-C-H	69.2	2	171	41.0	77	259
	750 rpm	PHB	115.6	3	171	16.9	0-50°C	274
High Shear Profile	250 rpm	PHB-H	77.2	3	172	40.0	76	261
	500 rpm	PHB-H	59.9	-1	169	40.9	75	264
	750 rpm	PHB-H	47.7	2	173	39.7	70	262
	250 rpm	PHB-C-H	74.9	3	168	39.6	76	259
	500 rpm	PHB-C-H	52.9	2	168	39.5	75	258
	750 rpm	PHB-C-H	43.4	1	165	40.5	74	257
	750 rpm	PHB-C-H	43.4	1	165	40.5	74	257

### 3.1.3. Thermal and crystallization behaviour

DSC analyses revealed that introducing hemp fibres drove to two concomitant effects on the crystallization behaviour of the matrix polymer (Table 1). First, a plasticizing effect was noticed

by a reduced glass transition temperature ( $T_g$ ) for PHB-H in comparison with PHB. This  $T_g$  reduction was limited ( $-4^\circ\text{C}$  was the largest  $T_g$  shift) and attributed to the production of PHB oligomers during processing. Indeed, the already reported strong diminution of mass-average molar mass indicated a shift of the molar mass distribution towards lower values and the apparition of PHB oligomers which acted as plasticizers of the PHB matrix. The second effect induced by the introduction of hemp fibres was a strong nucleating effect. Crystallinities of the unfilled extruded matrices were rather low (table1) while the biocomposites exhibited much higher  $X_c$  values, around 40%. An another clear evidence of the nucleation effect is the  $T_c$  shift towards high temperatures (table 1). Besides, DSC cooling curves of the unfilled materials hardly exhibited crystallization regions, between  $50^\circ\text{C}$  and  $0^\circ\text{C}$  in comparison with the biocomposites which presented clear crystallization peaks around  $75^\circ\text{C}$ . On heating DSC curves, unfilled materials exhibited cold crystallization peaks, which disappeared totally for the fibres-filled materials. This nucleating effect was already noticed visually during the biocomposites elaboration. At the extruder die, the melt material exhibited some rigidity whereas the unfilled material flew out of the extruder as a liquid. When the compatibilizer was used, the previously detailed plasticizing effect was slightly compensated by a reduction of the macromolecular mobility induced by improved fibre/matrix interactions and/or a better fibre dispersion (Table 1).

Concerning the thermal stability of the materials, the effect of the process was clear, as revealed by the degradation onset ( $T_{-5\%}$ ) provided in Table 1. The raw PHB pellets exhibited a degradation onset of  $279^\circ\text{C}$  which was slightly reduced down to  $274^\circ\text{C}$  after one extra extrusion step (high shear process). The drop was even higher for the low shear process ( $T_{-5\%} = 265^\circ\text{C}$ ). This sensitization provides from the extrusion step which led to random chain scissions [42] and creation of crotonate-ending PHB oligomers and crotonic acid [43]. Such reactions, confirmed by  $M_w$  measurements, contributed to reduce the thermal stability of the material.

However, the difference observed between the two extruded polymers may be linked to their crystalline content (16.9% for the high-shear extruded and 9.6% for the low-shear one). Indeed, in the highly ordered state exhibited by crystalline phases, it is less possible for macromolecules to move one relatively to another as additional forces must be overcome in the transformation to the unordered fluid state [44]. This energy difference was maintained after the polymer melting and appeared as a difference among degradation onsets. For the fibres-containing materials, the  $T_{-5\%}$  reduction was higher than the unfilled extruded PHB. Such results confirmed the fibre-induced sensitization previously discussed when detailing Mw results, the hemp fibres favoring the PHB hydrolysis and intensifying the internal warming of the matrix by increasing the melt-shear viscosity.

### **3.2. Mechanical properties**

Given the concomitant reductions of both Mw and thermal performances of the biocomposites when a compatibilizer was introduced and/or when high shear rates were applied during processing, the mechanical performances of the so-prepared materials were expected to be negatively impacted by these two processing parameters.

The effects induced by the processing conditions (screw speed and profile) were rather weak regarding the Young's modulus. Indeed, the stiffnesses of the various biocomposites prepared without compatibilizer (PHB-H) ranged between 304 and 336 MPa, without significant differences (figure 3). However, the processing conditions had a much clearer impact onto the ultimate properties and notably onto stress at break, which frankly decreased when the screw speed increased, from 33.9 MPa for PHB-H LS250 down to 29.5 MPa for PHB-H LS750. This drop was even higher for the material processed with the high-shear profile. The stress at break was reduced by 49% when the screw speed increased from 250 rpm to 750 rpm for PHB-H under high shear. Concomitantly the ductility of the materials was significantly reduced. Such

a trend can be explained as when the processing conditions became more severe antagonist phenomena occurred on fibre dispersion (positive), possible degradation of fibres (negative) and degradation of polymers (negative).

The introduction of compatibilizer significantly increased the materials' stiffness, and this load-transfer was more noticeable for the materials that stayed in the melt state for a longer time. For instance, the Young's modulus increased by 19%, 50% and 40% respectively when compatibilizer was added to PHB-H LS250, PHB-H LS500 and PHB-H LS750 respectively. The higher residence time induced by the low-shear process improved the transfer of the compatibilizer towards the fibre/matrix interface and finally drove to better compatibilization mechanisms, as observed when the materials underwent short strain levels. For higher strain levels, the addition of compatibilizer had fewer effect. Indeed, the stress at break was only slightly impacted, thus indicating that the fibre/matrix interfacial adhesion could still be improved.

Contrary to the clear trends observed for the low-shear processed materials, where coupling the fibres and the matrix was an efficient way to tune the mechanical performances, the results reported for the high-shear processed materials were unpredictable. This absence of correlation was attributed to the severe degradation mechanisms induced by the process, which deleted the influence of the compatibilizer.

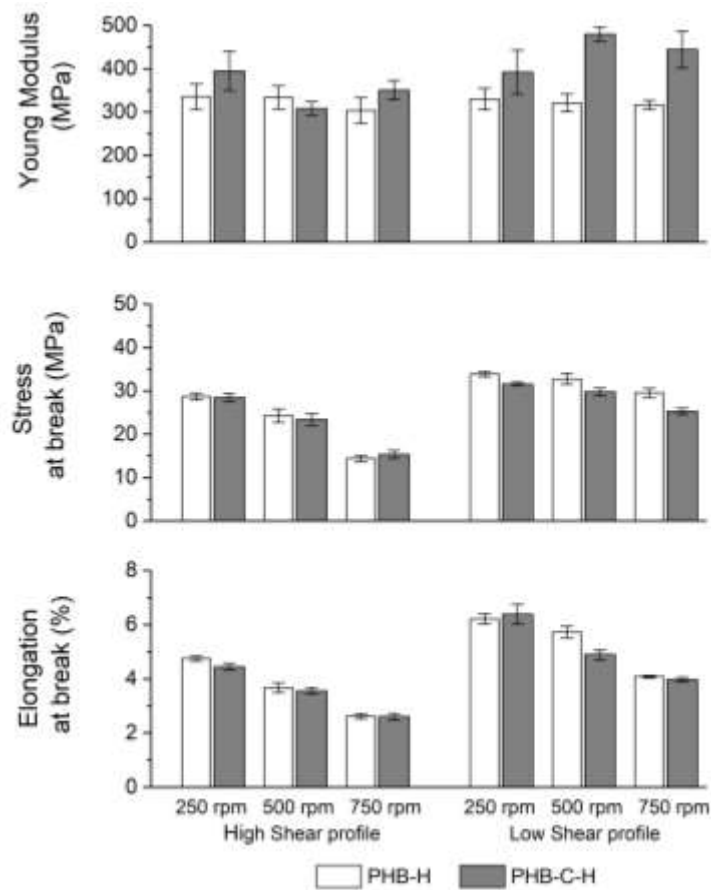


Figure 3. Tensile properties of PHB-based biocomposites

### 3.3. Water sensitivity

In addition to the mechanical performances, an extra aspect of the elaborated biocomposites was investigated, being a key property for the targeted packaging application. Transfer properties have been assessed by evaluating the water vapour permeation of the biocomposites

(figure 4) and by modelling the behaviour of the materials, the water vapour sorption parameters were obtained (table 2).

Table 2. Water vapour sorption fitted parameters obtained at 25°C

		D x 10 <sup>13</sup> (m <sup>2</sup> s <sup>-1</sup> )		moisture uptake at equilibrium (percentage of initial weight)	
		PHB-H	PHB-C-H	PHB-H	PHB-C-H
Low shear rate	250 rpm	4,0	1,4	2,7	2,9
	500 rpm	3,8	2,3	2,9	2,2
	750 rpm	3,3	2,8	3,5	2,0
High shear rate	250 rpm	3,9	3,7	3,1	2,8
	500 rpm	11,3	4,5	2,6	2,9
	750 rpm	11,6	5,3	2,2	3,1

The moisture content adsorbed by the materials at equilibrium was around 2 and 3% for all the composites, whatever the processing conditions and the composition. Similar results were provided by Stubar et al.[45] who reported that compatibilizing a PHB matrix with lignocellulosic fibres slowed moisture transport into the composites without modifying the equilibrium moisture content. The present equilibrium was linked to the hemp fibres (20 wt% content) which were much more sensitive to water vapour than the PHB matrix, which was reported to sorb at equilibrium less than 0.4 wt% moisture in similar conditions [33]. Moreover Christian and Billington [45] reported moisture contents at equilibrium for PHB/hemp biocomposites of 6.8 to 8.1% with 40 wt% fibre content, which is consistent with the values of the present work. In addition to the fibre content, the matrix degradation state and the presence of compatibilizer are considered as secondary parameters influencing the final moisture content. Despite the similar equilibrium observed, the kinetics observed to reach it, assessed by the water vapour diffusivity (D), highly depended on the process used to elaborate the material. And similarly to what has been observed for the mechanical properties, the water vapour sorption highly depended on the screw profile used for the elaboration. Notably, when the low shear profile was used, the influences of the screw speed and the composition were

clear. Indeed, by improving the dispersion state (through higher screw speed and the recourse to compatibilization) and the interphase quality (by adding a compatibilizer), the fibres were less percolating and better coated, which limited the diffusion of water vapour among the material. This reduction of the D value observed when a compatibilizer was introduced into the composition (table 2) was higher for the materials elaborated at low screw speed, i.e. with higher residence time enabling better compatibilization processes. For the composites elaborated under low shear, the D value reduced by 66% at 250 rpm, 40% at 500 rpm and 17% at 750 rpm when a compatibilizer was introduced. For the composites elaborated under high shear, the water vapour diffusions were much higher than when the low shear profile was used during the elaboration process. The whole resulting D values obtained by the various processing routes ranged from 1.4 to 11.6  $10^{-13} \text{ m}^2\text{s}^{-1}$  enabling the application as packaging materials to various food products.

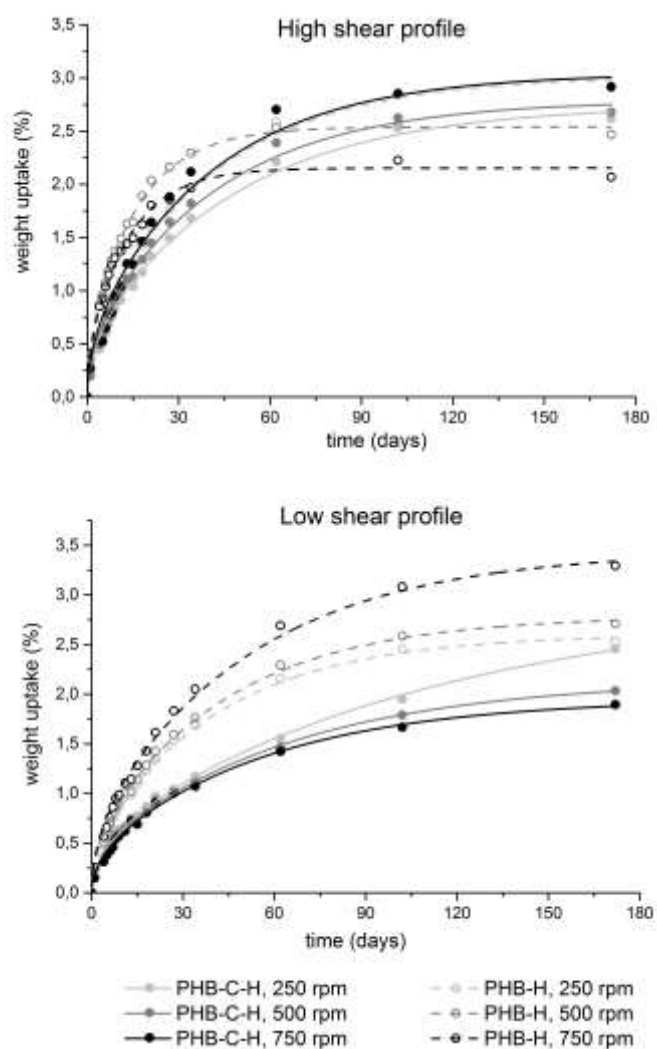


Figure 4. Water vapour sorption isotherm of biocomposites and fitted curves

### 3.4. Biodegradability

The end of life of the elaborated biocomposites has been assessed by respirometric tests held in compost conditions. Biodegradation patterns of two biocomposites (PHB-H LS250 and PHB-C-H HS750) are presented in figure 5, in addition with the one related to the pure PHB matrix.

The pure PHB material degraded faster than the reference (cellulose). Indeed, after a 27 days incubation, PHB exhibited around 80% of biodegradation while the reference underwent only 60% of biodegradation. Moreover, the addition of fibres did not impact negatively this high biodegradability, as indicated by the slightly higher biodegradation level exhibited by PHB-H after 92 incubation days (figure 5). This result is consistent with the literature [46] which reveals that the biodegradation of biocomposites containing lignocellulosic fibres is mainly driven by the ability of the matrix to biodegrade. As far as polyhydroxyalkanoates are concerned, the introduction of natural fibres was reported to improve the biodegradability of the composite in comparison with the pure matrix [6] by creating additional pathways for moisture, enzymatic, and microbial ingress leading to fibre swelling, increased damage at the fibre-matrix interface, and cracking, further accelerating degradation [47].

The introduction of compatibilizer drove to the highest biodegradation pattern (figure 5), even if not statistically different from the two other PHB-based materials. Introducing fibres and compatibilizer into the PHB matrix drove to the most severe Mw reduction and lead to the highest biodegradation level. This was highly consistent with the results provided by Hong et al. who reported that the presence of PHB oligomers increased the biodegradation rate of PHB [48]. All in all, whatever the composition and processing conditions, the biodegradation of the PHB-based biocomposites was revealed to be fast and high.

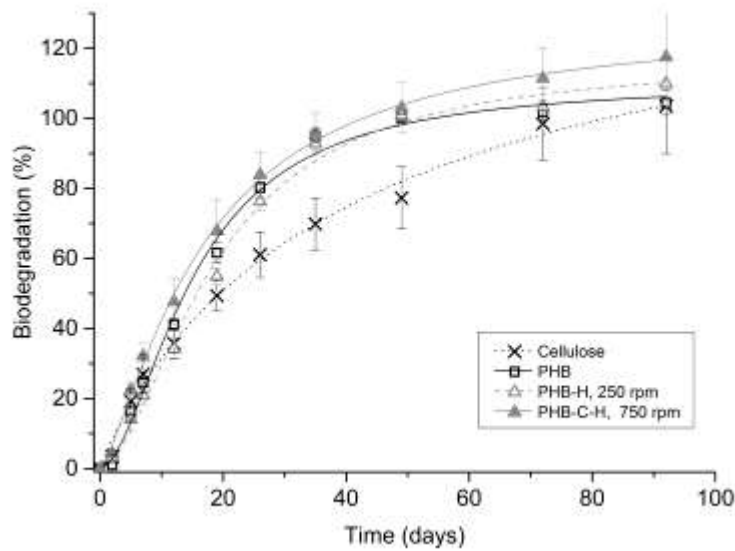


Figure 5. Biodegradation pattern of PHB-based materials in compost conditions

#### 4. Conclusion

Polyhydroxyalkanoates/hemp fibres biocomposites have been successfully prepared by reactive extrusion with various processing conditions, i.e variable shear rates (screw profile and speed) applied during the extrusion step and variable formulation (possible use of a compatibilizer). Structural analyses revealed homogeneous fibres dispersion states and the development of an interphase when a compatibilizer was introduced. Introducing fibres drove to two main effects concerning the processed matrix. First, the crystallization kinetics of the polymer strongly improved and made it unnecessary the usual recourse to nucleating agents. Second, the polymer matrix underwent some thermal sensitization. Indeed, in the case of severe processing conditions, the fibre dispersion state was improved but severe degradation reactions occurred at the same time, then hindering the possible improvement provided by the compatibilizer. For

the materials processed under low-shear rate, mechanical performances were preserved and even improved when the compatibilizer was added. All in all, the whole materials prepared under various processing routes presented a wide range of transfer properties and remained quickly and fully biodegradable. The original compatibilization route proposed here was confirmed and offers new opportunities to design biocomposites with tuned performances, reduced cost and low environmental impact.

## 5. Acknowledgements

The authors thank Carnot Institutes Carnot 3BCAR, Chimie Balard and ICEE for funding the present MACOBIO project under grant agreement number XXXXX.

## 6. References

1. Tokiwa, Y. and B.P. Calabia, *Degradation of microbial polyesters*. Biotechnology Letters, 2004. **26**(15): p. 1181-1189.
2. Zaverl, M., et al., *Studies on recyclability of polyhydroxybutyrate-co-valerate bioplastic: Multiple melt processing and performance evaluations*. Journal of Applied Polymer Science, 2012. **125**: p. E324-E331.
3. Serafim, L.S., et al., *Strategies for PHA production by mixed cultures and renewable waste materials*. Applied Microbiology and Biotechnology, 2008. **81**(4): p. 615-628.
4. Bugnicourt, E., et al., *Polyhydroxyalkanoate (PHA): Review of synthesis, characteristics, processing and potential applications in packaging*. Express Polymer Letters, 2014. **8**(11): p. 791-808.
5. Nielsen, C., et al., *Food waste conversion to microbial polyhydroxyalkanoates*. Microbial Biotechnology, 2017. **10**(6): p. 1338-1352.
6. Gunning, M.A., et al., *Mechanical and biodegradation performance of short natural fibre polyhydroxybutyrate composites*. Polymer Testing, 2013. **32**(8): p. 1603-1611.
7. Hermida, E.B. and V.I. Mega, *Transcrystallization kinetics at the poly(3-hydroxybutyrate-co-3-hydroxyvalerate)/hemp fibre interface*. Composites Part a-Applied Science and Manufacturing, 2007. **38**(5): p. 1387-1394.
8. Berthet, M.A., et al., *Exploring the potentialities of using lignocellulosic fibres derived from three food by-products as constituents of biocomposites for food packaging*. Industrial Crops and Products, 2015. **69**: p. 110-122.
9. Berthet, M.A., et al., *Sustainable food packaging: Valorising wheat straw fibres for tuning PHBV-based composites properties*. Composites Part a-Applied Science and Manufacturing, 2015. **72**: p. 139-147.

10. Reis, K.C., et al., *Particles of Coffee Wastes as Reinforcement in Polyhydroxybutyrate (PHB) Based Composites*. Materials Research-Ibero-American Journal of Materials, 2015. **18**(3): p. 546-552.
11. Wei, L.Q., S.B. Liang, and A.G. McDonald, *Thermophysical properties and biodegradation of green composites made from polyhydroxybutyrate and potato peel waste fermentation residue*. Industrial Crops and Products, 2015. **69**: p. 91-103.
12. Bledzki, A.K. and J. Gassan, *Composites reinforced with cellulose based fibres*. Progress in Polymer Science, 1999. **24**(2): p. 221-274.
13. Mohanty, A.K., M. Misra, and L.T. Drzal, *Surface modifications of natural fibers and performance of the resulting biocomposites: An overview*. Composite Interfaces, 2001. **8**(5): p. 313-343.
14. Belgacem, M.N. and A. Gandini, *The surface modification of cellulose fibres for use as reinforcing elements in composite materials*. Composite Interfaces, 2005. **12**(1-2): p. 41-75.
15. Gandini, A. and M.N. Belgacem, *Physical and chemical methods of fiber surface modification.*, in *Interface Engineering in Natural Fibre Composites for Maximum Performance.*, Z. N.E., Editor. 2011, Woodhead Publishing: Cambridge. p. 3-42.
16. Reddy, J.P., M. Misra, and A. Mohanty, *Renewable resources-based PTT poly(trimethylene terephthalate) /switchgrass fiber composites: The effect of compatibilization*. Pure and Applied Chemistry, 2013. **85**(3): p. 521-532.
17. Yu, L., K. Dean, and L. Li, *Polymer blends and composites from renewable resources*. Progress in Polymer Science, 2006. **31**(6): p. 576-602.
18. Bocque, M., et al., *Petro-Based and Bio-Based Plasticizers: Chemical Structures to Plasticizing Properties*. Journal of Polymer Science Part a-Polymer Chemistry, 2016. **54**(1): p. 11-33.
19. Samper-Madrigal, M.D., et al., *The effect of sepiolite on the compatibilization of polyethylene-thermoplastic starch blends for environmentally friendly films*. Journal of Materials Science, 2015. **50**(2): p. 863-872.
20. Wu, D. and M. Hakkarainen, *Recycling PLA to multifunctional oligomeric compatibilizers for PLA/starch composites*. European Polymer Journal, 2015. **64**: p. 126-137.
21. Xiong, Z., et al., *Preparation of Biobased Monofunctional Compatibilizer from Cardanol To Fabricate Polylactide/Starch Blends with Superior Tensile Properties*. Industrial & Engineering Chemistry Research, 2014. **53**(26): p. 10653-10659.
22. Jaillet, F., et al., *Synthesis of cardanol oil building blocks for polymer synthesis*. Green Materials, 2015. **3**(3): p. 59-70.
23. Benyahya, S., et al., *Functionalized green tea tannins as phenolic prepolymers for bio-based epoxy resins*. Industrial Crops and Products, 2014. **53**: p. 296-307.
24. Bjorsvik, H.R., *Fine chemicals from lignosulfonates. 1. Synthesis of vanillin by oxidation of lignosulfonates*. Organic Process Research & Development, 1999. **3**(5): p. 330-340.
25. Fache, M., et al., *Vanillin, a promising biobased building-block for monomer synthesis*. Green Chemistry, 2014. **16**(4): p. 1987-1998.
26. Pickering, K.L., M.G.A. Efendy, and T.M. Le, *A review of recent developments in natural fibre composites and their mechanical performance*. Composites Part a-Applied Science and Manufacturing, 2016. **83**: p. 98-112.
27. Faruk, O., et al., *Biocomposites reinforced with natural fibers: 2000-2010*. Progress in Polymer Science, 2012. **37**(11): p. 1552-1596.

28. Gamon, G., P. Evon, and L. Rigal, *Twin-screw extrusion impact on natural fibre morphology and material properties in poly(lactic acid) based biocomposites*. Industrial Crops and Products, 2013. **46**: p. 173-185.
29. Ranganathan, N., et al., *Effect of long fiber thermoplastic extrusion process on fiber dispersion and mechanical properties of viscose fiber/polypropylene composites*. Polymers for Advanced Technologies, 2016. **27**(5): p. 685-692.
30. Kuroda, M.M.H. and C.E. Scott, *Initial dispersion mechanisms of chopped glass fibers in polystyrene*. Polymer Composites, 2002. **23**(3): p. 395-405.
31. Cong, C.B., et al., *A study on properties of poly(3-hydroxybutyrate-co-4-hydroxybutyrate) with various 4HB contents and triethyl citrate plasticization*. Iranian Polymer Journal, 2008. **17**(1): p. 49-59.
32. Wolf, C., et al., *Water vapor sorption and diffusion in wheat straw particles and their impact on the mass transfer properties of biocomposites*. Journal of Applied Polymer Science, 2016. **133**(16).
33. Miguel, O. and J.J. Iruin, *Water transport properties in poly(3-hydroxybutyrate) and poly(3-hydroxybutyrate-co-3-hydroxyvalerate) biopolymers*. Journal of Applied Polymer Science, 1999. **73**(4): p. 455-468.
34. ASTM, *Standard Test Method for Moisture Absorption Properties and Equilibrium Conditioning of Polymer Matrix Composite Materials*. 2014: West Conshohocken, PA.
35. Shen, C.H. and G.S. Springer, *MOISTURE ABSORPTION AND DESORPTION OF COMPOSITE-MATERIALS*. Journal of Composite Materials, 1976. **10**(JAN): p. 2-20.
36. Lucas, N., et al., *Polymer biodegradation: Mechanisms and estimation techniques*. Chemosphere, 2008. **73**(4): p. 429-442.
37. Carrasco, F., et al., *Processing of poly(lactic acid): Characterization of chemical structure, thermal stability and mechanical properties*. Polymer Degradation and Stability, 2010. **95**(2): p. 116-125.
38. Pachekoski, W.M., C. Dalmolin, and J.A.M. Agnelli, *The Influence of the Industrial Processing on the Degradation of Poly(hydroxybutyrate) - PHB*. Materials Research-Ibero-American Journal of Materials, 2013. **16**(2): p. 327-332.
39. Montano-Herrera, L., et al., *In-line monitoring of thermal degradation of PHA during melt-processing by Near-Infrared spectroscopy*. New Biotechnology, 2014. **31**(4): p. 357-363.
40. Larsson, M., O. Markbo, and P. Jannasch, *Melt processability and thermomechanical properties of blends based on polyhydroxyalkanoates and poly(butylene adipate-co-terephthalate)*. Rsc Advances, 2016. **6**(50): p. 44354-44363.
41. Spitalsky, Z., et al., *Controlled degradation of polyhydroxybutyrate via alcoholysis with ethylene glycol or glycerol*. Polymer Degradation and Stability, 2006. **91**(4): p. 856-861.
42. Nguyen, S., G.E. Yu, and R.H. Marchessault, *Thermal degradation of poly(3-hydroxyalkanoates): Preparation of well-defined oligomers*. Biomacromolecules, 2002. **3**(1): p. 219-224.
43. Morikawa, H. and R.H. Marchessault, *PYROLYSIS OF BACTERIAL POLYALKANOATES*. Canadian Journal of Chemistry-Revue Canadienne De Chimie, 1981. **59**(15): p. 2306-2313.
44. Beyler, C.L. and M.M. Hirschler, *Thermal Decomposition of Polymers*, in *SFPE Handbook of Fire Protection Engineering*, Springer, Editor. 2002. p. 111-131.

45. Srubar, W.V., C.W. Frank, and S.L. Billington, *Modeling the kinetics of water transport and hydroexpansion in a lignocellulose-reinforced bacterial copolyester*. Polymer, 2012. **53**(11): p. 2152-2161.
46. Muniyasamy, S., et al., *Biodegradability and Compostability of Lignocellulosic Based Composite Materials*. Journal of Renewable Materials, 2013. **1**(4): p. 253-272.
47. Ryan, C., S. Billington, and C. Criddle, *Biocomposite Fiber-Matrix Treatments that Enhance In-Service Performance Can Also Accelerate End-of-Life Fragmentation and Anaerobic Biodegradation to Methane*. Journal of Polymers and the Environment, 2018. **26**(4): p. 1715-1726.
48. Hong, S.G., H.W. Hsu, and M.T. Ye, *Thermal properties and applications of low molecular weight polyhydroxybutyrate*. Journal of Thermal Analysis and Calorimetry, 2013. **111**(2): p. 1243-1250.